JOURNAL OF MATERIALS SCIENCE **37** (2002) 2077 – 2085

The crystallography and morphology of Mo_2C in ferrite

Y.-N. SHI, P.-M. KELLY*
Department of Mining, Minerals & Materials Engineering, The University of Queensland, St. Lucia, Brisbane, QLD 4072, Australia

The orientation relationships between hexagonal Mo_2C precipitates (H) in ferrite (B) have been determined by electron diffraction to an accuracy of $\pm 2^\circ$. With one exception, the 19 results are consistent with the previously reported Pitsch and Schrader (P/S) orientation relationship. However, these more accurate determinations show clearly that there is a systematic deviation of up to 5.5° from the exact P/S relationship and that this deviation consists of a small rotation about the parallel close packed directions-$[100]_B//[2\bar{1}\bar{1}0]_H$. The long direction of the Mo_2C needles has been determined unequivocally in terms of the orientation relationship to be $[100]_B//[2\bar{1}\bar{1}0]_H$. Moiré fringes between precipitate and matrix have been used to improve the accuracy of the orientation relationship results and to determine the lattice parameters of the carbide precipitates investigated. The Moiré fringe analysis has shown small systematic departures from the exact parallelism between $[100]_B$ and $[2\bar{1}\bar{1}0]_H$ along the length of Mo_2C needles and a lowering of the carbide lattice parameter that is consistent with the replacement of Mo by Fe in the carbide. The orientation relationship results, including the observed systematic deviation from the exact P/S relationship, are shown to be consistent with the edge-to-edge model.

1. Introduction

The orientation relationships (OR) between hexagonal carbides and nitrides (H) precipitated in a body centered cubic matrix (B) fall into two groups [1–3]. The first group is based on the Burgers OR [4], where the close packed directions in the two phases are parallel, i.e. $[1\bar{1}1]_B \parallel [2\bar{1}\bar{1}0]_H$. In the classic Burgers OR $(011)_B \parallel (0001)_H$. There are two other ORs that are related to this by a small rotation about $[1\bar{1}1]_B \parallel [2\bar{1}\bar{1}0]_H$. These are the Potter OR [5], where $(110)_B \parallel (01\bar{1}1)_H$ and the rotation angle is $\sim 2^\circ$ depending on the c/a ratio of the hexagonal phase, and the Jack OR [6] where both parallelisms—$(011)_B \parallel (0001)_H$ and $(110)_B \parallel (01\bar{1}1)_H$ are simultaneously obeyed (a condition that is only strictly true if $c/a = 1.5$). The other group of ORs have the directional parallelism $[100]_B \parallel [2\bar{1}\bar{1}0]_H$. The better known of these is the Pitsch/Schrader (P/S) OR [7] where $(011)_B \parallel (0001)_H$. The somewhat rarer Rong/Dunlop (R/D) OR [1, 2] is rotated about $[100]_B \parallel [2\bar{1}\bar{1}0]_H$ relative to the P/S OR by 18.4° to make $(021)_B \parallel (0001)_H$. Note that both the Burgers and the P/S ORs share the same plane parallelism—$(011)_B \parallel (0001)_H$—and are related by a 5.26° rotation about the normal to these parallel planes [2, 5]. This relatively small angular difference between the Burgers and P/S ORs, coupled with the limited accuracy of conventional selected area electron diffraction, has probably been responsible for confusion between these two quite distinct ORs. Nevertheless, it would appear that the Burgers OR and the very closely related Potter OR are restricted to systems with the lattice parameter ratio of the two phases (a_H/a_B) in the range 0.90 to 0.97, while those systems that have unequivocally been found to obey the P/S (or R/D) OR have $a_H/a_B > 1.0$ [5].

This behavior is consistent with the edge-to-edge matching model, which places considerable emphasis on the coincidence between close packed, or almost close packed, atom rows in the matrix and precipitate [8]. By analogy with the fcc/bcc system, which has already been analysed using edge-to-edge matching, the straight atom rows of importance are the $[2\bar{1}\bar{1}0]_H$ directions in the hcp structure (the equivalent of $[110]_F$ directions in the fcc structure) and the $[111]_B$ and $[100]_B$ directions in the bcc structure. The Burgers OR, with its close packed directional parallelism $[2\bar{1}\bar{1}0]_H \parallel [1\bar{1}1]_B$, is the hcp/bcc equivalent of the Kurdjumow/Sachs fcc/bcc OR [9]. In terms of the lattice parameters of the hcp and bcc phases, the atom spacing along these two rows will be the same when $a_H/a_B = 0.866$. If $a \pm 5\%$ variation in atom spacing can be tolerated in the corresponding atom rows, then the Burgers OR (and the associated Potter OR) would be expected to be observed in systems with a_H/a_B in the range 0.825 to 0.910. The P/S OR with its directional parallelism of $[100]_B \parallel [2\bar{1}\bar{1}0]_H$ is the fcc/bcc equivalent of the Nishiyama/Wassermann

*Author to whom all correspondence should be addressed.

OR [10, 11]. Using the same arguments as before and $a \pm 5\%$ variation in atom spacing, the P/S OR (and the associated R/D OR) would be expected to occur in systems with a_H/a_B in the range 0.95 to 1.05. The basic edge-to-edge matching concept and the correspondence between relatively close packed atom rows in the two structures seems to fit the observations of ORs in the hcp/bcc system. However, no systematic attempt has been made to date to apply the concept to the determination of detailed orientation relationships and morphology (habit plane of plates/laths and long directions of needles) in hcp/bcc systems. The purpose of the present work was to apply the edge-to-edge matching concept to one of the hcp/bcc systems and to evaluate the predictions using experimental data. The system chosen was the precipitation of Mo_2C in ferrite. This corresponds to a ratio a_H/a_B of $\approx$1.04 and indicates that ORs in the P/S group will be obeyed. The Mo_2C/ferrite system is relatively easy to study because the precipitates can be grown to a reasonable size and it should be possible to determine the various crystallographic parameters reasonably accurately.

1.1. Theoretical predictions

Starting with the parallelism between the direction $[100]_B$ and $[2\bar{1}\bar{1}0]_H$ the traditional edge-to-edge matching approach was followed. This suggested possible edge-to-edge matching between the following pairs of planes—$(011)_B$ and $(0002)_H$, $(011)_B$ and $(10\bar{1}1)_H$ or $(002)_B$ and $(10\bar{1}3)_H$. The first case with $(011)_B \parallel (0002)_H$ is the P/S OR and has a planar spacing mismatch of 17.7% at $a_H/a_B = 1.04$ and $c/a = 1.6$. The second case is rotated about 28.5° from the P/S OR, corresponds to $(0001)_H$ about 2° from $(013)_B$, and for the same values of a_H/a_B and c/a has a planar spacing mismatch of 12%. The third case is some 5° from the Rong/Dunlop OR, corresponds to $(0001)_H$ approximately parallel to $(035)_B$ and has a planar spacing mismatch of 6%.

None of these situations were particularly promising in terms of leading to a habit plane prediction—largely because of the large planar spacing mismatch of 6 to 17.7%. Attempts to derive a habit plane and a corresponding OR confirmed this. However, the correspondence between close packed (or almost close packed) rows of atoms that is the basic principle of edge-to-edge matching is equally valid for needle-like precipitates that do not show any obvious habit plane. In this case what is required is to maximize the matching of rows of atoms along the direction of the needle-like precipitate. This is equivalent to finding the minimum sized unit cell for a coincidence site lattice (CSL) made up of matching rows of atoms—an approach used very successfully by Rong and Dunlop to explain both the P/S OR and their newly discovered OR between Mo_2C and ferrite [2].

The combination of the edge-to-edge matching principle of corresponding atom rows in the two phases with the CSL approach was performed as follows. Views of the arrangement of the relatively close packed atom rows in the two structures as seen along $[2\bar{1}\bar{1}0]_H$ and $[100]_B$ were superimposed on each other and rotated relative to one another to identify positions that led to the maximum coincidence between atom rows in the two structures. This is essentially what was done by Rong and Dunlop [2]. The main difference in the present work is that a wider variety of relative orientations were explored and all of the parallel atom rows were included, not just those coinciding with the edges of the unit cells of the two lattices.

The three edge-to-edge plane matching cases discussed above were used as starting points, with $a_H/a_B = 1.04$ and $c/a = 1.5875$. Only those CSLs that exhibited better than 1 coincident row in 50 (i.e. >2% coincidence) were considered. For these cases the values of a_H/a_B and of c/a that were required for perfect matching were calculated. In some cases the CSL unit cells in the two phases were not exactly the same in shape and there was a difference in the angle between the two unit cell vectors. One feature that emerged on rare occasions was that the row matching led to a pair of interpenetrating CSL lattices. In these cases the number of matching rows was double that determined by the CSL unit cell of either pair.

At the exact P/S OR—i.e. $(011)_B \parallel (0001)_H$—2.86% (1 in 35) of the atom rows were coincident when $a_H/a_B = 1.0206$ and $c/a = 1.6166$. Rotating away from the exact P/S OR by 2.04° about the parallel atom rows $[100]_B \parallel [2\bar{1}\bar{1}0]_H$ led to slightly better atom row matching of 3.08% (2 in 65) at $a_H/a_B = 1.0408$ and $c/a = 1.5751$. Further rotation to a point 5.56° from the exact P/S OR gave the best atom row matching of 4.17% (1 in 24). In this case $a_H/a_B = 1.0308$ and $c/a = 1.6315$, but the axial angles of the two CSL unit cells differed by ~0.6°. The R/D OR, which is rotated by 18.43° from the exact P/S OR, is the only other case that has identical axial angles, with atom row matching of 2.27% (1 in 44) at $a_H/a_B = 1.0328$ and $c/a = 1.5877$. All the other matching cases had differences in axial angles ranging from 0.22° to 0.82°.

The seven promising cases are illustrated in Fig. 1. Selecting the most appropriate for Mo_2C in ferrite depends on maximizing the degree of row matching at $a_H/a_B = 1.0375$ and $c/a = 1.5875$ (the values for Mo_2C in ferrite) and minimizing any differences in axial angles. Near the exact P/S position, the case tilted 2° away from P/S is probably the best. Further tilting leads to increased %ge row matching, but a larger difference in axial angle and less appropriate values of a_H/a_B and c/a. The R/D case at a tilt of 18.43° from exact P/S is also quite good, although the degree of atom row matching is less than the near P/S cases. Hence, the theoretical predictions of the edge-to-edge matching approach suggest that the two ORs observed for Mo_2C in ferrite should be either close to P/S (possibly tilted off exact P/S by ~2°) or the R/D OR, with the near P/S OR favoured over R/D because of the increased atom row matching—a prediction entirely consistent with observations [1, 12]. For both ORs the morphology of the precipitates should be needles lying along the parallel directions $[100]_B \parallel [2\bar{1}\bar{1}0]_H$—again consistent with previous observations [1, 12].

The purpose of the present work was to determine the ORs between Mo_2C in ferrite as accurately as possible,

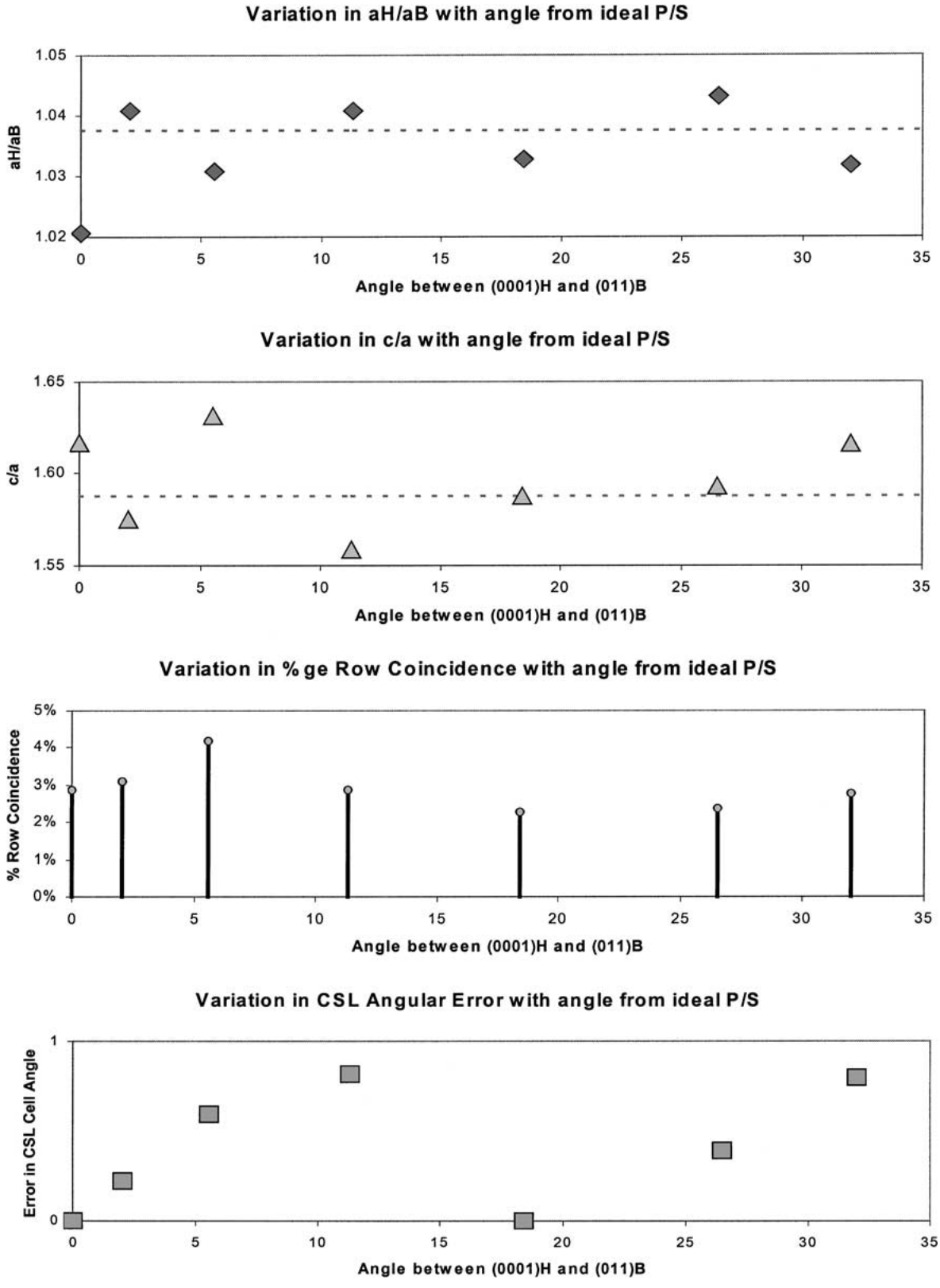

Figure 1 The seven possible ORs predicted by edge-to-edge matching.

in the hope of identifying any deviation from the exact P/S OR, and to see whether any other ORs, such as R/D, were observed. A subsidiary purpose was, where possible, to utilize Moiré fringes to determine a_H/a_B accurately and to estimate any small angular deviations between the planes giving rise to the Moiré fringes [13, 14]. Finally the morphology of the precipitate particles was carefully investigated and the long direction of the needles established in terms of the OR between the two phases—not just in terms of the matrix alone.

2. Experimental procedure

A steel of composition Fe-4.0wt%Mo-0.20wt% C was used in this work. The bar-shaped cast ingot was forged into a strip and then homogenized in an argon

atmosphere at 1300°C for about 1h and brine quenched. Subsequently it was aged at 710°C for up to 10 hours. 3 mm diameter disks were punched from the strip and jet polished in an 8% perchloric and acetic acid solution at 30 V. The foils were examined in a JEOL 2010 transmission electron microscope at 200 kV. The lattice parameters of Mo_2C and ferrite were determined by X-ray diffraction.

As the Mo_2C precipitates were completely embedded in the foil, it was impossible to get good Kikuchi line patterns from them. The orientation relationships were therefore determined by conventional selected area diffraction (spot) patterns. However, to improve accuracy and remove the ambiguity of indexing, the method proposed by Ryder and Pitsch [15, 16] was employed. This makes use of particularly strong spots in the selected area diffraction (SAD) patterns and is capable of achieving an accuracy of orientation better than $\pm 1^\circ$.

3. Experimental results

3.1. Lattice parameters from X-ray diffraction

The lattice parameters determined from the diffractometer traces gave the following results.

$$Mo_2C\ a_H = 0.2977\,\text{nm}; \quad c_H = 0.4726\,\text{nm};$$
$$c_H/a_H = 1.588$$
$$\text{Ferrite}\ a_B = 0.2861\,\text{nm}; \quad a_H/a_B = 1.0405$$

The Mo_2C data agrees very well with the results reported by Dyson *et al.* [12].

3.2. Orientation relationship

Fig. 2a shows a typical view of a foil aged at 710°C for 10 h. The Mo_2C particles lying in three directions are needle-shaped and 50 nm to 200 nm long. Overall 20 diffraction patterns from different areas were used to determine the OR between the Mo_2C precipitates and the ferrite matrix.

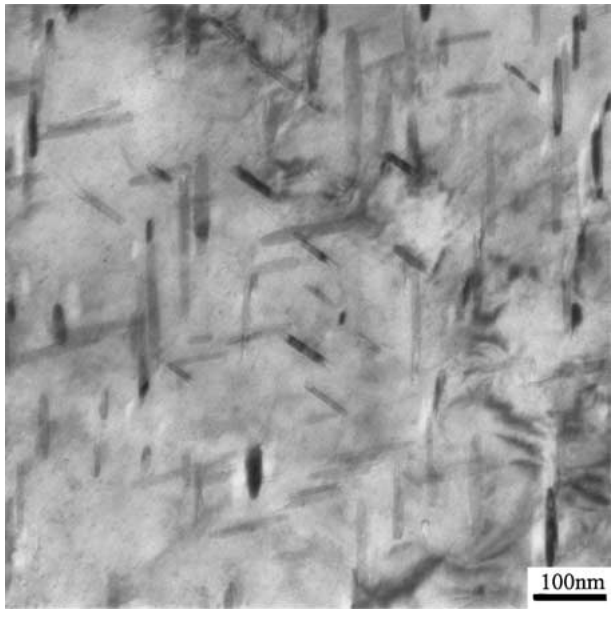

Figure 2 Transmission electron microphotograph of Mo_2C distributing in ferrite.

Fig. 3c shows the diffraction patterns taken from an area containing two Mo_2C needles shown in bright field in Fig. 3a and in dark field image (Fig. 3b). Fig. 3d gives the solution to this pattern. In this case the zone axes of the hexagonal Mo_2C and the bcc ferrite are $[22\bar{4}3]_H$ and $[120]_B$ respectively. The subscript B represents ferrite and H the Mo_2C. After using the method proposed by Ryder and Pitsch [15, 16], the zone axis of ferrite was found to be very close to $[250]_B$, i.e. the real zone axis was 4.6° away from $[120]_B$. In all cases, the orientations corrected via the Ryder/Pitsch method were used to determine the ORs between Mo_2C and ferrite.

In 19 of the 20 cases analysed the OR between Mo_2C and ferrite was close to the P/S OR:

$$[100]_B // [2\bar{1}\bar{1}0]_H$$
$$(011)_B // (0001)_H$$

This is illustrated on the stereographic projection in Fig. 4.

Fig. 5a and b show two enlarged regions of the stereographic projection in Fig. 4. The Ryder/Pitsch method gives an accuracy of $\pm 1^\circ$ for the orientation determinations from SAD spot patterns. Hence, the OR determination between two phases should be accurate to within $\pm 2^\circ$. Dotted circles representing this level of accuracy are indicated on Fig. 5a and b. This shows that for the directional parallelism of $[100]_B // [2\bar{1}\bar{1}0]_H$, 13 of the 19 OR determinations are within $\pm 2^\circ$ of the exact P/S OR, and none of the results is further than 3° from the exact P/S OR. The relationship between $(011)_B$ and $(0001)_H$ shown in Fig. 5b is somewhat different. Only one third of the OR determinations are within $\pm 2^\circ$ of the exact P/S OR and the others are spread out in the $(2\bar{1}\bar{1}0)_H$ plane by up to 5.5°.

3.3. The long direction

Trace analysis to determine the long direction of Mo_2C particles in terms of the both phases was performed on 13 pairs of electron micrographs and the corresponding diffraction patterns. In determining morphological characteristics of precipitate particles—i.e. the long direction of the Mo_2C needles in this case—it is important to perform the determination in terms of both phases. Determining the long direction as $\langle 100 \rangle_B$ in terms of the ferrite matrix and assuming that because $[100]_B // [2\bar{1}\bar{1}0]_H$ this is also the $[2\bar{1}\bar{1}0]_H$ direction is not enough to give an unequivocal determination. In the P/S OR only one of the $\langle 100 \rangle_B$ directions is parallel to $\langle 2\bar{1}\bar{1}0 \rangle_H$. The other two $\langle 100 \rangle_B$ directions in the matrix are within 2.32° of $\langle 01\bar{1}2 \rangle_H$ directions in the P/S OR. Hence, to obtain meaningful results, it is essential to determine the long direction of the Mo_2C needles in terms of both phases—i.e. in terms of variant of the OR for the particular Mo_2C needle (or group of needles) analysed. In all cases the OR was close to the P/S OR and the traces could be plotted on the standard variant of the OR shown in Fig. 4. The trace analysis was

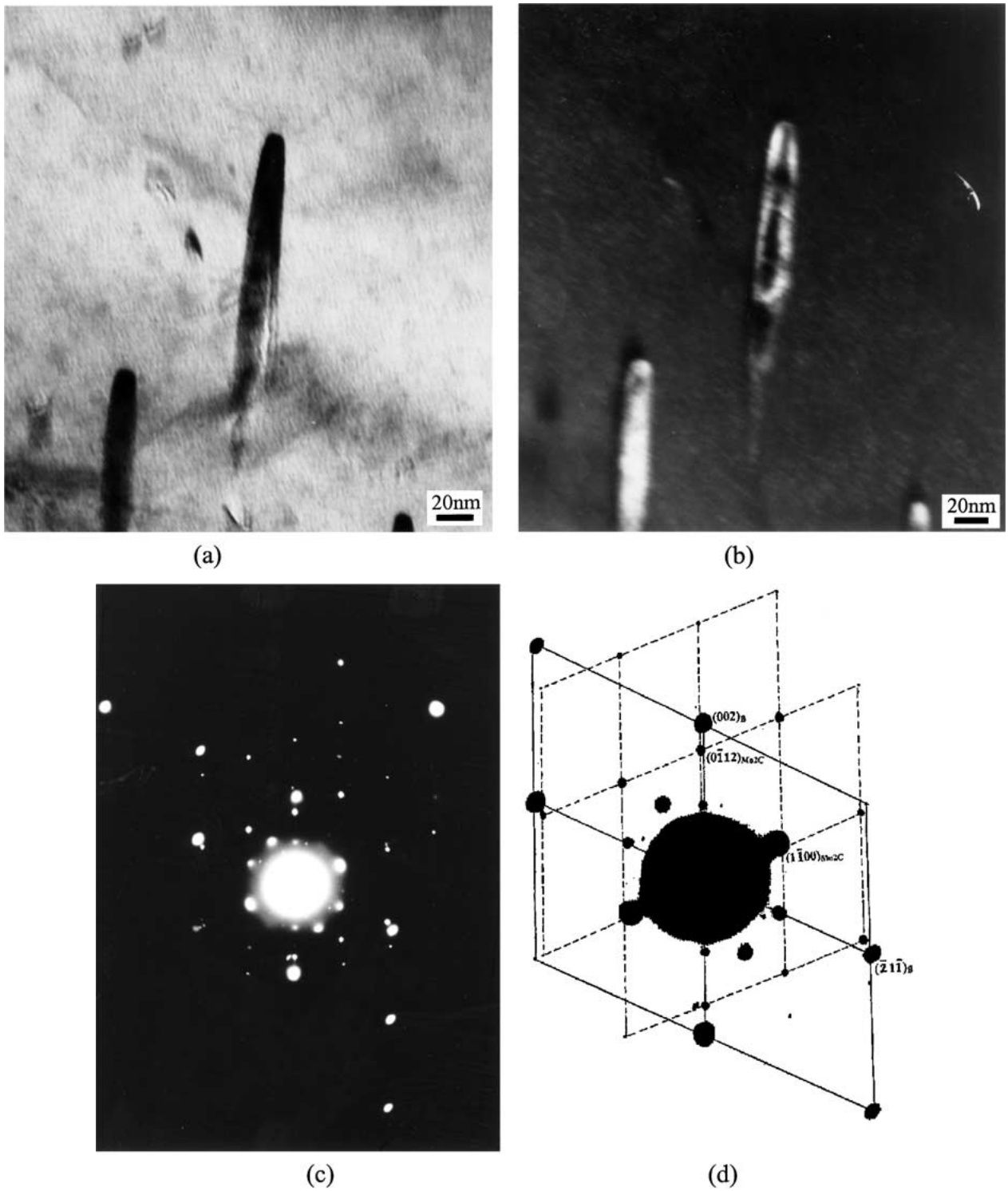

Figure 3 (a) Bright field image of area containing a pair of Mo_2C needles. (b) Corresponding dark field of (a) taken with a [22$\bar{4}$3] Mo_2C reflection. (c) Diffraction pattern of the area shown in (a) and (b). (d) Solution to the diffraction pattern in (c) with dotted lines outlining the hexagonal Mo_2C pattern and heavy lines the body-centered cubic ferrite pattern.

performed by calculating the trace direction (OT) of the needles in terms of both phases. As shown in Fig. 6, if OT was inclined at angle α to the vector $\mathbf{g}_A$ defining spot A in the diffraction pattern and at angle β to the vector $\mathbf{g}_B$ defining spot B in the pattern, then $\mathbf{t}'$ (the unit vector of OT) is given by:

$$\mathbf{t}' = \frac{\mathbf{g}'_A \sin\beta + \mathbf{g}'_B \sin\alpha}{\sin(\alpha+\beta)} \qquad (1)$$

where $\mathbf{g}'_A$ is the unit vector parallel to $\mathbf{g}_A$ (i.e. parallel to OA) and $\mathbf{g}'_B$ is the unit vector parallel to $\mathbf{g}_B$ (i.e. parallel to OB). Note that this analysis can be performed in terms of both the Mo_2C and the ferrite patterns. The cross product of $\mathbf{t}'$, and a unit vector parallel to the beam ($\mathbf{z}'$)—i.e. $\mathbf{t}' \wedge \mathbf{z}'$—gives a direction $\mathbf{n}'$ normal to the long direction of the needle.

If the particles are actually needles then $\mathbf{n}'$ should always lie 90° from the needle axis. This is illustrated in Fig. 7a, where it is clear that all 13 results are close to 90° from $[100]_B // [2\bar{1}\bar{1}0]_H$.

Fig. 7b shows the conventional traces analysis for the 13 determinations (the trace of the plane containing $\mathbf{z}'$ and $\mathbf{n}'$) plotted in terms of the two phases—i.e. in terms

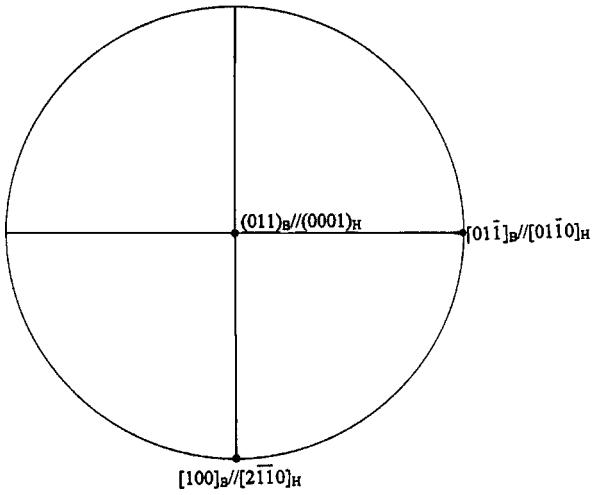

Figure 4 Stereographic projection of Mo_2C and ferrite that obeys P/S OR.

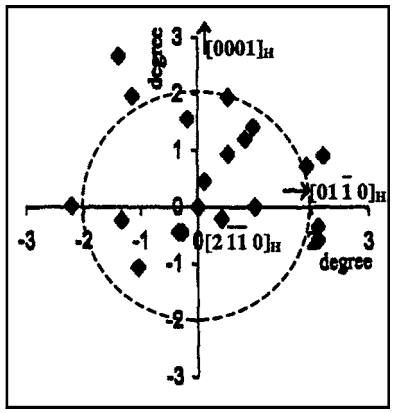

(a)

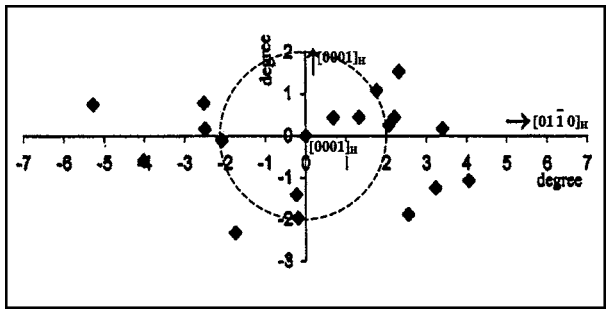

(b)

Figure 5 (a) Enlarged region of a stereographic projection near $[2\bar{1}\bar{1}0]_H$ showing the position of the experimental points. (b) Enlarged region of a stereographic projection near $[0001]_H$ showing the position of the experimental points.

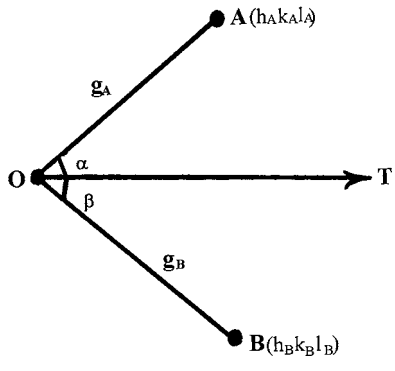

Figure 6 Illustration of the trace calculation.

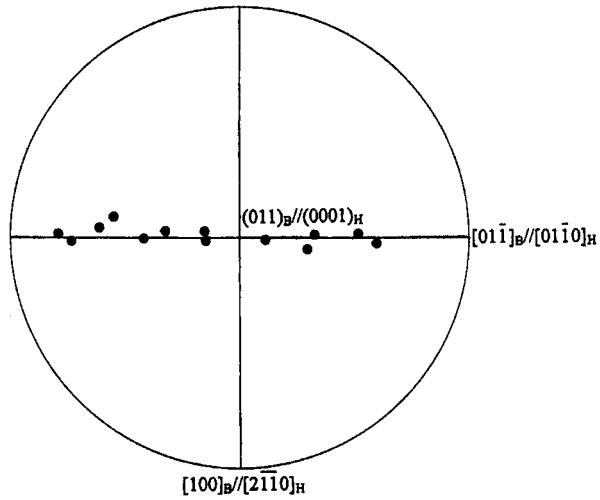

(a)

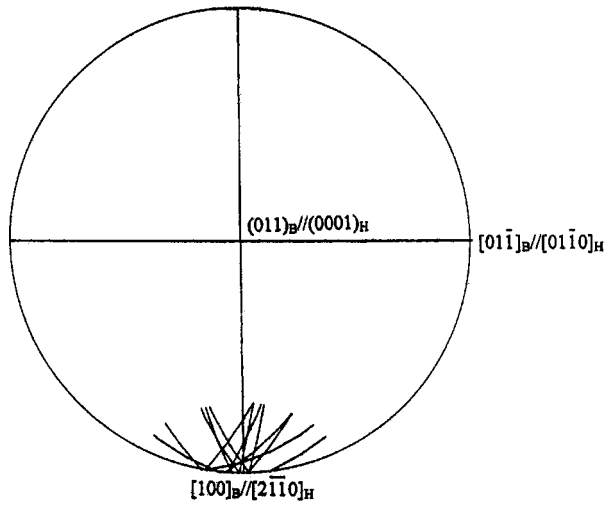

(b)

Figure 7 (a) The direction $\mathbf{n}'$ in the foil plane that are perpendicular to the traces of the Mo_2C needles. (b) Trace analysis of the long direction of Mo_2C in ferrite.

of the standard variant of the P/S OR. These results again clearly demonstrate that the long direction of the Mo_2C needles is $[100]_B//[2\bar{1}\bar{1}0]_H$.

To check that the Mo_2C was actually needle-like, the poles of the trace direction OT were plotted on the stereographic projection. If these defined a plane then this would correspond to the habit plane of a plate like particle. In fact the plots of the trace direction OT in terms of the variant of the P/S OR were scattered all over the projection and did not define a plane. This confirmed that the Mo_2C particles were needles.

3.4. Moiré fringes at the interface

Moiré fringes can provide information about the relative d-spacings and angular deviation between almost parallel planes in the two phases. In the general case, when two sets of reflecting planes in two phases are super-imposed, the Moiré fringe spacing D is given by [13]:

$$D = \frac{d_1 d_2}{\sqrt{d_1^2 + d_2^2 - 2d_1 d_2 \cos\phi}} \qquad (2)$$

Where d_1, d_2 are the d-spacings of the two planes respectively and ϕ is the angle between the two planes.

The angle of the fringes relative to the normal of the plane with spacing d_1 is given by

$$\sin\theta = \frac{d_1 \sin\phi}{\sqrt{d_1^2 + d_2^2 - 2d_1 d_2 \cos\phi}} \tag{3}$$

These two equations involve three unknowns, d_1, d_2 and ϕ. Although these three unknowns can be measured on the diffraction patterns, the accuracy is not adequate to give meaningful results—particularly at small values of ϕ. Since the one parameter that should be essentially constant is the matrix (ferrite) lattice parameter, then by making d_1 correspond to a matrix plane and rearranging Equations 2 and 3 it is possible to calculate ϕ and the ratio d_2/d_1. The accurate value of ϕ is useful in determining the orientation relationship between ferrite and Mo_2C. The ratio d_2/d_1 allows d_2 to be calculated from the value of d_1 (assumed to be fixed) and for a given c/a ratio the lattice parameter a_H/a_B can be derived.

The rearranged versions of Equation 2 and 3 for the case where $d_1 < d_2$ are:

$$\tan\phi = \frac{\sin\theta}{\frac{D}{d_1} - \cos\theta} \tag{4}$$

$$\frac{d_2}{d_1} = \frac{1}{\cos\phi - \sqrt{\cos^2\phi + (d_1/D)^2 - 1}} \tag{5}$$

Fig. 8a shows an example of Moiré fringes from $(200)_B$ and $(2\bar{1}\bar{1}0)_H$. The fringes are parallel to each other and are perpendicular to the long direction of the particle—i.e. $\phi = 0$. However the spacing of the Moiré fringes changes along the length of the particle. Table I gives the values of a_H and a_H/a_B calculated with an assumed lattice parameter of ferrite $a_B = 0.2861$ nm.

TABLE I Some results from the Moiré fringes from $(2\bar{1}\bar{1}0)_H$ and $(200)_B$

Measured		Calculated		
D(nm)	$\theta(^\circ)$	$\phi(^\circ)$	a_H/a_B	%Fe
5.143	0	0	1.029	22.1
4.857	0	0	1.030	20.2
4.571	0	0	1.032	18.1
3.810	0	0	1.039	11.0
3.714	0	0	1.040	9.8
3.619	0	0	1.041	8.7
3.143	0	0	1.048	1.7

Fig. 8b is a similar set of Moiré fringes from $(200)_B$ and $(2\bar{1}\bar{1}0)_H$ in another Mo_2C particle. At one end of the particle the fringes are perpendicular to the long direction of the particle, but begin to rotate away from this position at the other end. This indicates a progressive variation in ϕ from zero to $\sim 0.75^\circ$ along the length of the particle—see Table II. Note the magnifying effect in the Moiré fringe rotation, which is $\sim 30^\circ$ for every 1° change in ϕ.

Finally, Fig. 8c and d are bright and dark field images of the Moiré fringes from $[101]_B$ and $[1\bar{1}01]_H$. In this case and 6 other examples analysed, the fringes are equally spaced and oriented across the whole particle. The values of ϕ and a_H/a_B (assuming $c/a = 1.5875$) are

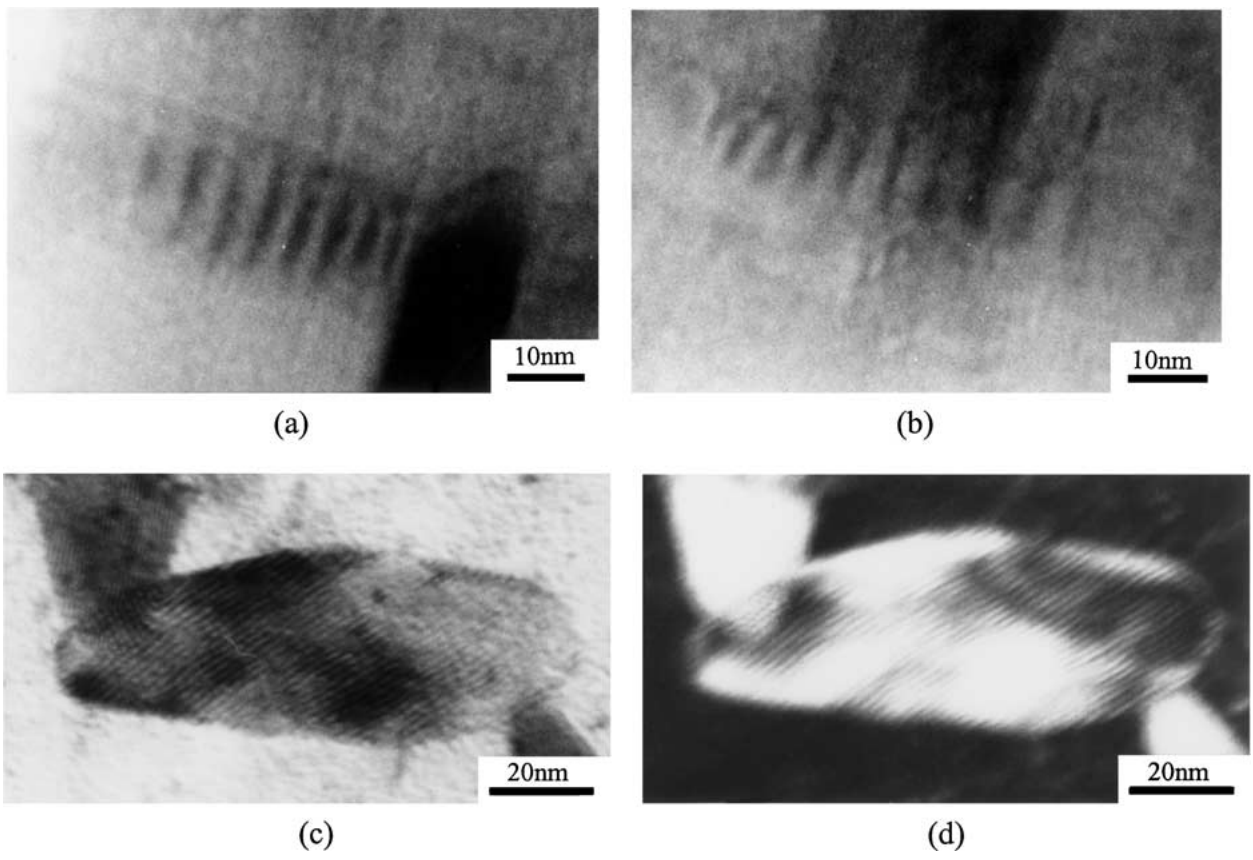

Figure 8 (a) and (b) Moiré fringes taken from $[200]_B$ and $[2\bar{1}\bar{1}0]_H$, (c) Bright field image of Moiré fringes taken from $[101]_B$ and $[1\bar{1}01]_H$, (d) Dark field image in the same area as (c).

TABLE II Changes of ϕ with the change of measured θ of Moiré fringes taken from $(2\bar{1}\bar{1}0)_H$ and $(200)_B$

Measured		Calculated		
D(nm)	$\theta(^\circ)$	$\phi(^\circ)$	a_H/a_B	%Fe
5.700	0	0	1.026	25.1
5.430	0	0	1.027	23.7
5.050	0	0	1.029	21.5
4.570	0	0	1.032	18.1
4.286	5.2	0.18	1.034	15.9
3.905	10.5	0.40	1.037	12.8
3.810	14.5	0.56	1.038	12.4
3.334	17.0	0.75	1.043	7.0

TABLE III Comparison of the calculated and measured angles of Moiré fringes taken from $[101]_B$ and $[1\bar{1}01]_H$

Measured			Calculated		
D(nm)	$\theta(^\circ)$	$\phi(^\circ)$	$\phi(^\circ)$	a_H/a_B	%Fe
1.790	40.0	4.0	4.55	1.015	36.6
2.188	19.0	2.0	1.89	1.019	32.7
1.938	14.0	2.0	1.61	1.035	15.7
1.549	33.0	4.4	4.57	1.041	8.7
1.788	42.5	4.0	4.77	1.011	40.6
1.750	27.0	4.0	3.35	1.035	15.1
1.470	45.0	6.0	6.15	1.024	26.5

shown in Table III, where the calculated ϕ values can be compared with those measured from the diffraction pattern. The agreement is generally within $\pm 0.75^\circ$.

4. Discussion

Nineteen of the twenty patterns analysed indicated an orientation relationship that was close to the P/S OR. The experimental error in these determinations was estimated to be approximately $\pm 2^\circ$. The parallelism between $[100]_B$ and $[2\bar{1}\bar{1}0]_H$ (Fig. 5a) was essentially consistent with this level of accuracy, but the experimentally determined angles between $(011)_B$ and $(0001)_H$ showed a systematic deviation in the $(200)_B//(2\bar{1}\bar{1}0)_H$ plane of up to $\pm 5.5^\circ$—well in excess of the $\pm 2^\circ$ experimental error (see Fig. 5b). This indicates a few degrees systematic deviation from the exact P/S OR that corresponds to a rotation about $[100]_B//[2\bar{1}\bar{1}0]_H$. This was entirely consistent with the prediction in Fig. 1, where two of the near P/S ORs correspond to rotations about $[100]_B//[2\bar{1}\bar{1}0]_H$ of 2° and 5.5° respectively.

Finally it is worth noting that only one of the 20 patterns analysed gave a result significantly away from the P/S OR. In this single case the experimental OR was 32° away from the exact P/S OR and coincided with the predicted OR on the far right of Fig. 1. The Rong/Dunlop OR was not observed in the present work.

The trace analysis results from 13 particles (all in terms of the OR) confirmed that the particles were needle-like with a long axis parallel to $[100]_B//[2\bar{1}\bar{1}0]_H$.

The Moiré fringe technique has shown that it can give very accurate values for the angle ϕ between planes in the two phases. What was unexpected was the rotation of the $(200)_B//(2\bar{1}\bar{1}0)_H$ Moiré fringes in one isolated case (Fig. 8a). This indicated a real variation in the OR along the length of the particle (ϕ up to 0.75° from the expected value of 0°). The other unexpected result from the Moiré fringe analysis was that the value of a_H/a_B was often well below the expected value for pure Mo_2C in ferrite and that on occasions (Tables I and II) there were clear variations in a_H/a_B along the length of a single particle. A possible explanation for a_H/a_B being less than the expected value is the substitution Fe for Mo in the carbide. By assuming that this would lead to a linear reduction in a_H/a_B with increasing Fe content the value of x in the carbide formula $(Fe_xMo_{(1-x)})_2C$ can be calculated from a_H when $x = 1.0$(a_H for ε-carbide $= 0.2734$) and a_H for pure Mo_2C ($x = 0$). The %Fe content calculated in this way is given in Tables I to III for each of the Moiré fringe spacing. These values are probably only accurate to ± 5%Fe, but they are sufficiently large to indicate a real variation in Fe content (from 0 to 40%) in different particles (Table III) and a systematic increase in Fe content from the end of the particle ($\sim$0% Fe) to the centre (25% Fe). The reason for this variation within a single particle is not understood.

5. Conclusions

1. Of the 20 SAD patterns analysed, 19 were within 5.5° of the P/S orientation relationship.

2. The deviations from exact P/S OR consistent of a rotation of up to 5.5° about the common axis $[100]_B//[2\bar{1}\bar{1}0]_H$.

3. The Rong/Dunlop OR was not observed, but a single OR corresponding to a rotation of 32° about $[100]_B//[2\bar{1}\bar{1}0]_H$ was found.

4. The particles were always needle-like with the long direction parallel to $[100]_B//[2\bar{1}\bar{1}0]_H$.

5. Apart from the absence of the Rong/Dunlop OR, the results in (1) to (3) above are entirely consistent with the edge-to-edge matching approach.

6. Analysis of the Moiré fringes between the Mo_2C particles and the ferrite matrix showed that:

(a) Moiré fringes provide a very accurate measurement of the angle ϕ between the planes giving rise to the fringes and this can assist in improving the accuracy of OR determinations.

(b) In one case a real deviation (up to 0.75°) from the exact parallelism between $[100]_B$ and $[2\bar{1}\bar{1}0]_H$ occurred along the length of a particle.

(c) The values of the a_H/a_B were often lower (never higher) than expected from pure Mo_2C in ferrite. This has been interpreted as being due to substitution of Fe for Mo in the carbide.

(d) In two cases (Fig. 8a and b) there appeared to be a progressive change in a_H/a_B along the length of a single carbide particle. This corresponded to the centre of the particle being essentially pure (Fe-free) Mo_2C, while the tip had a higher Fe content.

Acknowledgement

The work described in this paper was supported by an Australia Research Council (ARC) Small Grant. The authors are most grateful for this support.

References

1. RONG WANG and G. L. DUNLOP, *Acta Metall.* **32** (1984) 1591.
2. RONG WANG, G. L. DUNLOP and K. H. KUO, *ibid.* **34** (1986) 681.
3. D. DULY, *Acta Metall. Mater.* **41** (1993) 1559.
4. W. G. BURGERS, *Physica* **1** (1934) 561.
5. D. I. POTTER, *J. Less Common Metals* **31** (1973) 299.
6. K. H. JACK, *J. Iron Steel Inst.* **169** (1951) 26.
7. W. PITSCH and A. SCHRADER, *Arch. Eisenhütt Wes.* 29 (1958) 715.
8. P. M. KELLY and M.-X. ZHANG, in *Mater. Forum*, Australia, 1999, p. 41.
9. G. V. KURDJUMOW and G. Z. SACHS, *Physik* **64** (1930) 325.
10. Z. NISHIYAMA, *Sci. Rep. Tohoku Univ.* **23** (1934) 638.
11. G. WASSERMANN, *Arch. Eisenh.* **16** (1933) 647.
12. D. J. DYSON, S. R. KEOWN, D. RAYNOR and J. A. WHITEMAN, *Acta Metall.* **14** (1966) 867.
13. P. HIRSCH, A. HOWIE, R. NICHOLSON, D. W. PASHLEY and M. J. WHELAN, in "Electron Microscopy of Thin Crystals" (Butterworths, London, 1965) p. 311.
14. A. KUMAR and B. L. EYRE, *Acta Metallurgica* **26** (1978) 569.
15. P. L. RYDER and W. PITSCH, *Phil. Mag.* **15** (1967) 437.
16. *Idem.*, *ibid.* **18** (1968) 807.

Received 11 January 2001
and accepted 16 January 2002